High-pressure structure and equation of state study of nitrosonium nitrate from synchrotron x-ray diffraction

Yang Song[a)]
Geophysical Laboratory, Carnegie Institution of Washington, Washington, D.C. 20015, and Department of Chemistry and Chemical Biology, Harvard University, Cambridge, Massachusetts 02138

Maddury Somayazulu, Ho-kwang Mao, and Russell J. Hemley
Geophysical Laboratory, Carnegie Institution of Washington, Washington, D.C. 20015

Dudley R. Herschbach
Department of Chemistry and Chemical Biology, Harvard University, Cambridge, Massachusetts 02138

(Received 1 November 2002; accepted 20 February 2003)

Several nitrogen oxide compounds transform to nitrosonium nitrate ($NO^+NO_3^-$) under high pressure. In this study, $NO^+NO_3^-$ was synthesized by laser heating of N_2O in a diamond-anvil cell and characterized by x-ray diffraction as a function of pressure at room temperature and low temperature. The unit-cell parameters were refined up to 32.2 GPa at 300 K, resulting in a denser structure than reported previously. The pressure-volume relations for $NO^+NO_3^-$ at 300 K were fitted to both Birch-Murnaghan and Vinet equations of state. The analysis indicates that $NO^+NO_3^-$ is denser than other nitrogen-oxygen assemblages, consistent with the conclusion that formation of the ionic species is driven by density rather than entropic effects. The low-temperature x-ray-diffraction data represent the first *in situ* measurements for this material, revealing consistent structural information and evolutions under pressure. These observations provide additional information on the stability relations and reaction diagram of N_2O and $NO^+NO_3^-$. © *2003 American Institute of Physics.* [DOI: 10.1063/1.1566939]

I. INTRODUCTION

The stability of nitrosonium nitrate ($NO^+NO_3^-$) in condensed phase has received considerable attention over the past two decades. The formation of $NO^+NO_3^-$ was first observed by infrared spectroscopy of oxidized NO by Parts *et al.*[1] $NO^+NO_3^-$ was also found to occur as the isomer of molecular N_2O_4 trapped in a neon matrix.[2] In later Raman spectroscopy studies of solid N_2O_4, Bouldan *et al.*[3] showed that temperature-induced autoionization produced $NO^+NO_3^-$. In these ambient pressure studies, $NO^+NO_3^-$ appears to be stable only at low temperatures. However, Angew and co-workers[4,5] found that molecular N_2O_4 could be transformed into ionic $NO^+NO_3^-$ either by photolysis or pressure at room temperature. For instance, laser irradiation of cubic Im 3 α-N_2O_4 results in the formation of β-N_2O_4 with an unknown noncubic structure at 1.16 GPa at room temperature.[4,5] At pressures of 1.5–3.0 GPa at room temperature, β-N_2O_4 exhibits a reversible phase transition with a large hysteresis to ionic $NO^+NO_3^-$.[4,5] Despite the observation of $NO^+NO_3^-$ on various occasions, its structure has remained unknown until recently. Somayazulu *et al.*[6] discovered that at 10–30 GPa and 1000–2000 K, N_2O transforms to nitrosonium nitrate via the reaction, $4N_2O \rightarrow NO^+NO_3^- + 3N_2$. An orthorhombic structure for $NO^+NO_3^-$ was proposed based on angle dispersive x-ray diffraction in a diamond-anvil cell at a single pressure of 21 GPa. Iota *et al.*[7] observed a similar transformation of N_2O to $NO^+NO_3^-$ at high pressure and high temperatures, but details of the results have not been published.

In order to better understand the properties and structures of $NO^+NO_3^-$, we have obtained additional x-ray-diffraction measurements over a broad range of pressures and temperatures. These data complement an extended spectroscopic investigation of $NO^+NO_3^-$ over a similar P-T range using Raman and infrared spectroscopy.[8] We report here x-ray-diffraction data for $NO^+NO_3^-$ at pressures up to 32.2 GPa. The diffraction patterns are consistent with the orthorhombic symmetry found previously at a single pressure[6] but with the more complete data obtained here provides a more reliable structural model that gives a denser phase. The cell parameters are fitted to both Birch-Murnaghan and Vinet equations of state.[9,10] The density of the ionic compound $NO^+NO_3^-$ is compared with that of various oxygen-nitrogen assemblages. This study, together with our recent spectroscopic results[8] enables a stability diagram for $NO^+NO_3^-$ to be constructed.

II. EXPERIMENT

Samples were prepared in Mao-Bell diamond-anvil cells with large optical openings on both sides (>30°) to facilitate x-ray-diffraction measurements. Pure N_2O (99%, Aldrich)

a)Author to whom correspondence should be addressed. Electronic mail: ysong@chemistry.harvard.edu

was loaded into the diamond cell cryogenically as described previously.[8] Ruby chips were added to the sample chamber to enable pressures to be determined by the shift of the R_1 ruby fluorescence line.[11] The accuracy of the pressure measurements was ± 0.05 GPa under hydrostatic conditions.

The pressurized N_2O sample (above 10 GPa) was heated by means of a CO_2 infrared laser (10.6 μm) to drive the reaction to form $NO^+NO_3^-$. The laser output power was about 50 W and the estimated temperature attained was between 1000 and 2000 K with the laser spot focused to 50 μm. The transformation of N_2O to $NO^+NO_3^-$ was confirmed by Raman spectroscopy, particularly by the appearance of the strong NO^+ stretching mode at 2240 cm^{-1}, the ν_4, ν_2, and ν_1 modes of NO_3^-, as well as abundant lattice modes at low frequencies. The samples were taken to beamline X17C at National Synchrotron Radiation Source (NSLS) at Brookhaven National Laboratory (BNL) for x-ray-diffraction measurements. The beamline instrumentation and diffraction geometry have been described previously.[12] For each measurement, the cell was oscillated along ω and χ to minimize the effects of preferred orientation and 2θ was fixed at 8.99°. The diffraction pattern was calibrated with diffraction lines of gold. Background was subtracted at each pressure before indexing diffraction peaks. We collected nine x-ray-diffraction patterns from 9.9 to 32.2 GPa.

In order to locate more accurately the pressure of the phase transition[8] that occurs below 10 GPa, we also obtained low-temperature *in situ* x-ray measurements using a cryostat at beamline X17B. The sample was cooled to 80 K using liquid nitrogen and x-ray-diffraction data were collected with a 2θ angle usually at 10.0°. No oscillation of the cell was performed due to the spatial constraints imposed by the cryostat.

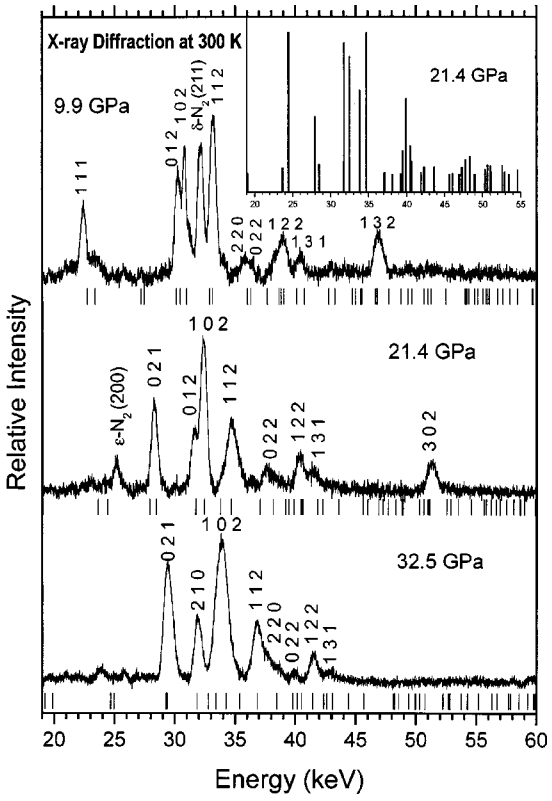

FIG. 1. Energy dispersive x-ray-diffraction pattern of $NO^+NO_3^-$ measured at (a) 9.9 GPa, (b) 21.4 GPa, and (c) 32.2 GPa and room temperature. Background has been subtracted. The energy calibration was obtained from a gold external standard diffraction pattern and the pattern has been background subtracted. The 2θ used was 8.99°. The calculated d spacings are indicated below each diffraction pattern. The calculated intensity profile for the energy-dispersive x-ray-diffraction pattern at 21.4 GPa is shown in the inset.

III. RESULTS

A. Room-temperature x-ray diffraction

Figure 1 shows typical diffraction patterns for pressures of 9.9, 21.4, and 32.2 GPa. The assignments of the major peaks arising from $NO^+NO_3^-$ diffraction are labeled. By tracing the major peaks, the diffraction patterns can be consistently assigned at all pressures. The conversion from energy to d spacings was based on the well-known relation[12] $d(\text{Å}) = 6.1993/[E(\text{keV})\sin\theta]$. The peak identified as $hkl = 102$ is among the most prominent observed at all pressures (except 16.5 GPa); other major peaks such as 021, 012, and 112 are observed at most pressures.

In general, only peaks in the energy range between 27 and 45 keV are analyzed; in that range, all major peaks are observed for each pressure. On the low-energy side (below 27 keV) corresponding to high d spacing, peaks observed at certain pressures, such as 9.9 and 21.4 GPa, are not consistently observed at other pressures, such as 32.5 GPa [Fig. 1(c)]. The peak at 22.4 keV at 9.9 GPa can be assigned as the 111 diffraction line of $NO^+NO_3^-$ while that at 25.2 keV at 21.4 GPa is closest to ε-N_2 200 (see below). At high energy (low d spacing), assignment of some peaks may not be unique due to more than one possible (hkl) combination. For example, the peaks observed at 46.9 keV (1.69 Å) and 51.3 keV (1.54 Å) at 9.9 and 21.4 GPa could be assigned most closely to 132 and 302, respectively. Such peaks were not used to fit the cell parameters due to the possibility of contribution from nearby diffraction lines. Between 27 and 45 keV, all peaks are found to be associated with $NO^+NO_3^-$ diffraction, with the exception that at some pressures (especially low pressures) some peaks are attributed to N_2 diffraction. N_2 crystallizes in the disordered cubic δ phase (space group $Pm3n$) at pressure of 5–16 GPa at room temperature, transforming to the ordered rhombohedral ε phase ($R\bar{3}c$) above 16.4 GPa.[13] The peak observed at 30.8 keV (2.57 Å) at 9.9 GPa is most likely the 211 of δ-N_2. Because of congestion in the pattern and the lower resolution of the energy-dispersive diffraction, some weak diffraction lines at certain pressures are obscured by adjacent strong lines, such as 021 and 211 at 9.9 GPa, 220 at 21.4 GPa, and 012 and 211 at 32.5 GPa. In such situation, these lines are either not labeled or resolved by careful deconvolution.

In the previous x-ray-diffraction study carried out at a single pressure of 21 GPa,[6] diffraction due to ε-N_2 was identified and the remaining peaks of $NO^+NO_3^-$ were indexed to give an orthorhombic unit cell with cell parameters $a = 5.658$ Å, $b = 7.324$ Å, and $c = 6.202$ Å, and $V = 257.7$ Å^3. The systematic extinctions in the diffraction pattern suggested space groups $Pmcn$ or $P2_1cn$, similar to the arago-

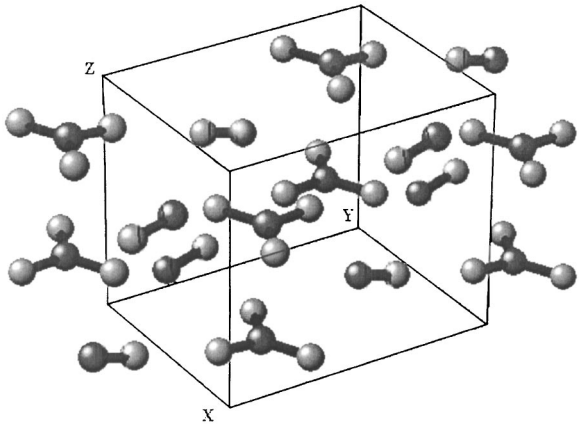

FIG. 2. Proposed structure model of $NO^+NO_3^-$ (see text).

nite phase of $CaCO_3$ and KNO_3. In the analysis of our new data, the indices of the peaks observed at all pressures likewise suggest the point group of $mm2$ with a primitive cell. The coincidence of the Raman and IR lines indicates a noncentrosymmetric cell and therefore $P2_1cn$. If the observed hkl at all pressures are combined, we find all possible hkl associated with space group $P2_1cn$ appear, except for 200; evidently, that peak is uniformly weak. A proposed structure containing four NO^+ and NO_3^- pairs is shown in Fig. 2. This overall topology is consistent with first-principles calculations; for example, in the calculated low-energy structure the NO bond points to the center of NO_3.[14]

There are differences in both the intensity distribution and observed diffraction lines between the current and previously measured diffraction patterns; there are also differences between the patterns measured here. These differences forced us to perform a comprehensive analysis of all patterns, including a careful re-analysis of previous data. The combination of the patterns measured near 21 GPa using the two techniques allowed us to obtain an improved fit to the previously obtained pattern, with unit-cell parameters $a=5.66(2)$ Å, $b=6.47(2)$ Å, and $c=5.39(1)$ Å at 21.0 GPa. This is consistent with the parameters from the current data set $a=5.60(1)$ Å, $b=6.55(1)$ Å, and $c=5.41(2)$ Å at 21.4 GPa. The results give a denser structure than previously reported.[6] The new analysis is based on a more extensive data set and is more reliable. Unfortunately, the intensities in the diffraction data cannot be used quantitatively for structure analysis. The predicted pattern at 21 GPa assuming space group $P2_1cn$ and the aragonite structure is shown (Fig. 1 inset). Despite the strong mismatch of the intensity of 020 at 24.4 keV, reasonably good matches between the experimental and the fitted are found for all other major diffraction lines especially in the region between 27 and 45 keV. Furthermore, now the d spacings can be consistently indexed at all other pressures. The major d spacings as a function of pressure are shown in Fig. 3.

Because of the preferred orientation of the sample, the intensity of each diffraction peak can vary dramatically even for two adjacent pressures. As mentioned above, the intensity profile was not used for any quantitative analysis. To determine the unit-cell parameters, only those dominant peaks

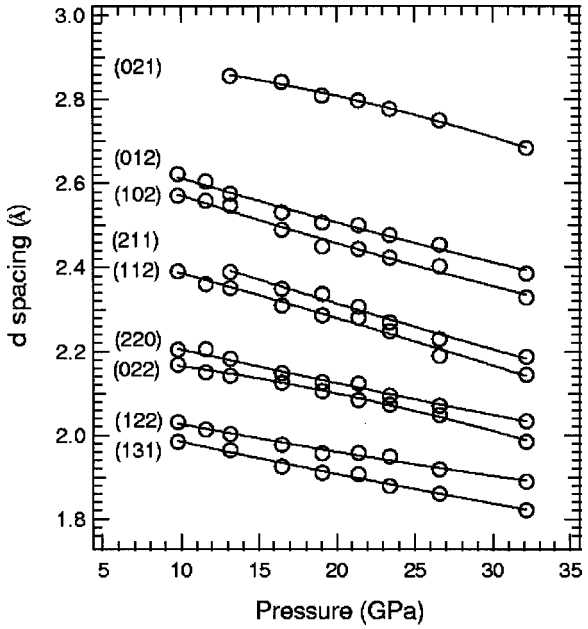

FIG. 3. Principal d spacings observed as a function of pressure. The solid lines are to guide the eye to show the evolution of d spacings on pressure.

with unique and traceable identities are used. The unit-cell parameters are listed in Table I. In indexing the peaks, we specified $a<c<b$ to avoid confusion due to the permutation of axes. We find that the compressibility differs for the three axes. From 9.9 to 32.5 GPa, the a, b, and c axes are compressed by 6%, 7%, and 8%, respectively. However, the pressure dependences of the axial ratio are found to be relatively constant. From 9.9 to 32.5 GPa, b/a varies from 1.17 to 1.18, while c/a fluctuates between 0.97 and 0.99.

B. Equation of state

The unit-cell volume was calculated from the orthorhombic cell parameters (Table I); the molecular volume was determined assuming each cell containing four molecules ($Z=4$). The room-temperature P-V relations for $NO^+NO_3^-$ is plotted in Fig. 3. Also shown is the data point from the new refinement of the earlier study at 21 GPa. Although $NO^+NO_3^-$ has been investigated by several groups, to our knowledge information about its compressibility has not

TABLE I. Cell parameters for $NO^+NO_3^-$ determined by x-ray diffraction (300 K).

Pressure (GPa)	a (Å)	b (Å)	c (Å)	V (Å^3/cell)
9.9	5.76(1)	6.76(2)	5.69(1)	221.6(1.0)
11.6	5.71(1)	6.72(4)	5.61(1)	215.3(1.2)
13.2	5.65(1)	6.69(2)	5.57(1)	210.5(1.3)
16.5	5.65(3)	6.67(2)	5.52(2)	208.0(1.2)
19.1	5.61(2)	6.57(1)	5.44(2)	200.5(1.6)
21.4	5.60(1)	6.55(1)	5.41(2)	198.3(2.2)
23.4	5.54(1)	6.50(1)	5.40(1)	194.4(0.9)
26.3	5.46(3)	6.37(2)	5.34(3)	185.7(1.0)
32.2	5.41(3)	6.29(1)	5.24(1)	178.3(1.2)

been published. An important aim of this study was therefore to establish an equation of state for $NO^+NO_3^-$.

The compression data for $NO^+NO_3^-$ were fit to a Birch-Murnaghan equation of state (EOS):[9]

$$P=\frac{3}{2}K_0\left[\left(\frac{V_0}{V}\right)^{7/3}-\left(\frac{V_0}{V}\right)^{5/3}\right]\cdot\left\{1-\frac{3}{4}(4-K_0')\left[\left(\frac{V_0}{V}\right)^{2/3}-1\right]\right\}, \quad (1)$$

where P and V are pressures and volumes, K_0 and K_0' the bulk modulus and its first derivative at a given temperature. The subscript denotes a reference state, taken as ambient (zero) pressure. The Birch-Murnaghan equation can be recast as

$$K=\frac{2}{3}P\left[\left(\frac{V_0}{V}\right)^{7/3}-\left(\frac{V_0}{V}\right)^{5/3}\right]^{-1}=K_0-\frac{3}{4}K_0(4-K_0')\left[\left(\frac{V_0}{V}\right)^{2/3}-1\right], \quad (2)$$

where K is the bulk modulus along the P-V curve. Least-squares fit gives V_0 as 265.0(±2.0) Å^3/cell, with $K_0=45.2$ (±0.9) GPa and $K_0'=3.18(\pm 0.90)$. Note that K_0' is often found to be close to 4 for many materials.[15] For highly compressible materials such as molecular solids, the Vinet *et al.*[10] function has been shown to provide a better representation of the EOS.[18] This function has an exponential form,

$$P=3K_0\left(1-\frac{V}{V_0}\right)\left(\frac{V}{V_0}\right)^{-2/3}\exp\left[\frac{3}{2}(K_0'-1)\left(1-\frac{V}{V_0}\right)\right]. \quad (3)$$

Using this formula and the V_0 used in the Birch-Murnaghan equation, least-squares fits of the data give $K_0=42.3$ ±1.0 GPa and $K_0'=3.52\pm 0.60$, very close to those obtained with the second-order Birch-Murnaghan EOS. The results of both fits are shown in the figure.

Figure 4 also shows the room-temperature P-V relations for O_2, N_2, and N_2O. At 300 K, O_2 is a supercritical fluid below 5.5 GPa and crystallizes in the rhombohedral β phase (space group $R\bar{3}m$) at 5.5–11 GPa.[19] Above 11 GPa, O_2 forms the ε phase to the maximum pressures studied here.[19] Solid N_2 undergoes several pressure-induced phase transitions ($\beta\rightarrow\delta\rightarrow\varepsilon$) at room temperature (not evident in the plot). Also shown is the volume of the assemblage of one N_2 and two O_2 molecules, an equivalent stoichiometric assemblage of $NO^+NO_3^-$.

The zero-pressure molecular volumes for N_2 and O_2 are 45 Å^3 (Ref. 13) and 40.2 Å^3 (Ref. 16). The molecular volume for $NO^+NO_3^-$ is 66.25 Å^3 as compared to the volume of the assemblage N_2+2O_2 of 125.4 Å^3. The unit-cell volume for molecular N_2O_4 (isomer of $NO^+NO_3^-$) has been determined by single-crystal diffraction measurement at −40 °C and ambient pressure.[17] The cubic unit cell (space group $Im3$, $Z=6$) has a cell parameter $a=7.77$ Å, or 78.18 Å^3/molecule, 18% larger than the fitted zero-pressure volume for $NO^+NO_3^-$ obtained here. Moreover, $NO^+NO_3^-$ is denser than the assemblage at all pressures studied here. We note that the previous comparison[6] with N_2+2O_2 used the EOS

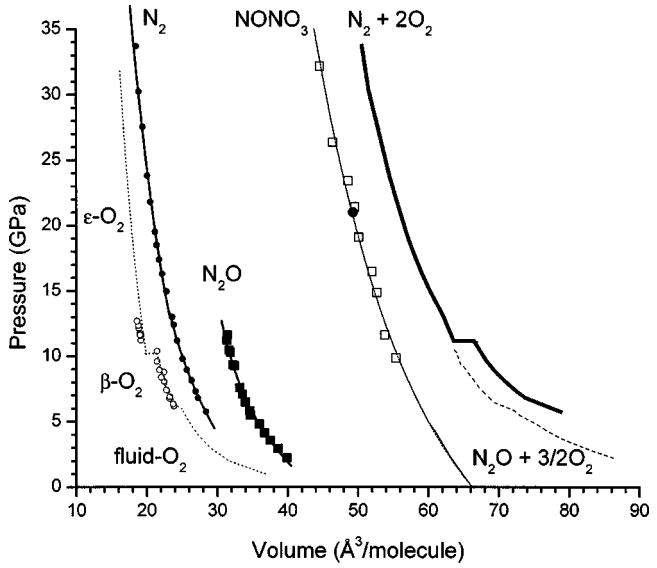

FIG. 4. Pressure-volume relations for $NO^+NO_3^-$ and other molecular systems. (□) $NO^+NO_3^-$ determined from the present energy-dispersive x-ray diffraction and that (●) from previous angle-dispersive x-ray diffraction with refined cell parameters compared with a third-order Birch-Murnaghan (——) and Vinet *et al.* EOS fits (-·-). For O_2 (···) data, below 5.5 GPa are for fluid O_2 (Ref. 31); above 5.5 GPa for the solid (Ref. 16). Experimental data for O_2 (○) at several pressures performed from Ref. 19 are also plotted. For N_2 (●), experimentally determined EOS is from Ref. 13, for N_2O (■) from (Ref. 22). Also shown are the corresponding volumes of stoichometrically equivalent assemblages of N_2+2O_2 (——) and $N_2O+3/2O_2$ (— — —).

of O_2 reported in Ref. 20. The cell volume of O_2 was more reliably determined in single-crystal x-ray-diffraction measurements by Johnson *et al.*[21] These data fall on the EOS plotted in Fig. 4. The combination of the reanalyzed cell parameters reported previously together with those obtained here indicates that $NO^+NO_3^-$ is a denser phase than the N_2 and O_2 assemblage. The P-V relation of N_2O derived from x-ray diffraction by Mills *et al.*[22] is also plotted. It can be seen that $NO^+NO_3^-$ is also denser than $N_2O+3/2O_2$.

C. Low-temperature x-ray diffraction

Our previous Raman spectra of $NO^+NO_3^-$ unambiguously identified a phase transition at 5 GPa and room temperature.[8] This led us to perform *in situ* x-ray-diffraction measurements at 80 K. Figure 5 shows the patterns collected at several selected pressures. The experiment was conducted by decompression starting at 11 GPa. At that pressure, in order to measure as many diffraction peaks as possible, several 2θ angles were used. Superimposed diffraction spectra converted from different 2θ angles in the energy dispersive scale to d-spacing plots proved to be consistent in terms of the peak positions, although the intensity distribution differs for different 2θ angles. The peaks were indexed by comparison with room-temperature patterns obtained at 11.6 GPa. Diffraction data above 34 keV were not used in the analysis because most arise from the steel gasket and others correspond to low d spacings not significant for characterization of the unit-cell parameters.

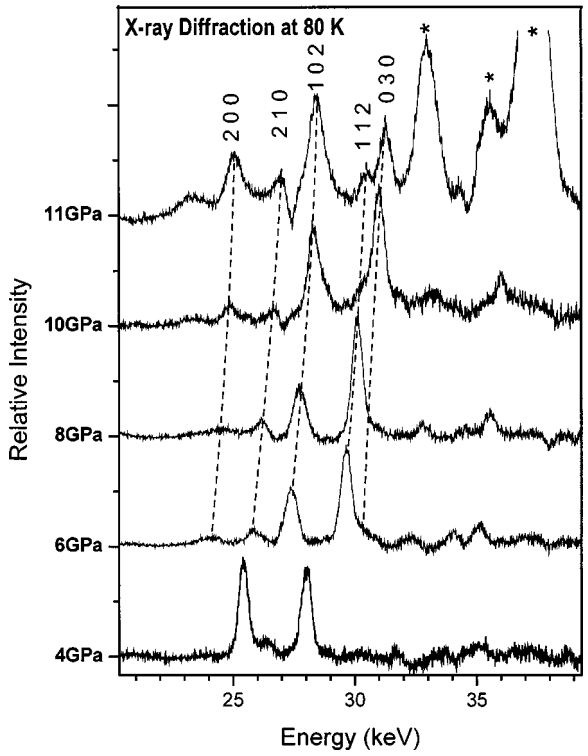

FIG. 5. X-ray-diffraction patterns of $NO^+NO_3^-$ measured *in situ* at 80 K and a series of decreasing pressures. The energy scale was calibrated using an external Au standard with $2\theta=10°$. The dotted lines are guides to the eye. The asterisks (*) denote the diffraction lines (100, 002, and 101) from the stainless steel gasket.

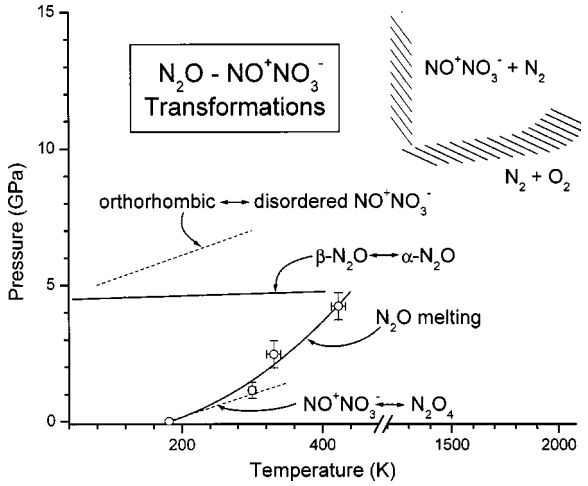

FIG. 6. Schematic phase and reaction diagram of $NO^+NO_3^-$ and N_2O. The boundary (——) between the α-($Pa3$) and β-($Cmca$) phases of N_2O is from Ref. 22. The phase boundary between α and fluid is indicated by open circles (present study) and solid line (fitted by Simon-type equation on data from both current measurements and Ref. 24). The approximate P-T regime for the transformation of N_2O into $NO^+NO_3^-$ or N_2 and O_2 is indicated by shaded lines (\\\); see also Ref. 8. The stability fields of other possible low P-T phases of N_2O are not shown. The boundary (···) between ionic $NO^+NO_3^-$ and molecular N_2O_4 is from previous spectroscopic measurements (Ref. 8). The approximate boundary (···) for the transformation (which may be gradual) between the orthorhombic $NO^+NO_3^-$ and disordered $NO^+NO_3^-$ was estimated from the diffraction patterns measured at low temperatures and room temperature (see text and Fig. 5).

Although the intensity varies for some diffraction lines from one pressure to another (mostly attributed to preferred orientation), d spacings follow a smooth pattern from 11 to 6 GPa. At each pressure, in general, two peaks are the most prominent. However, due to the longer collection time at 11 GPa, additional diffraction lines are evident, including diffraction lines the gasket. In the subsequent patterns measured at lower pressures the position of the sample was adjusted, resulting in a significant reduction in contamination of the pattern by the gasket. At 11 and 10 GPa, the 102 and 030 are prominent. At 8 and 6 GPa, the 102 peak persists but the intensity of the 030 decreases and the 112 peak becomes more prominent. This is again most probably associated with preferred orientation. In addition, the 210 and 200 are consistently observed. Just as at room temperature, at 80 K the observation of the 102 peak remained strong.

When the pressure was further released from 6 to 4 GPa, a significantly different diffraction pattern was obtained. The two most prominent peaks do not match the 102 and 112 lines documented at 6 GPa and are substantially shifted. In addition, other diffraction features likewise differ markedly from those observed at higher pressures. As in the room-temperature x-ray measurements, when the pressure is low enough (i.e., 2 GPa), no diffraction patterns were observable even with long exposure times. We conclude that $NO^+NO_3^-$ undergoes a phase transition at 80 K between 6 and 2 GPa, traversing intermediate structures such as that observed at 4 GPa. When combined with the room-temperature observation of a phase transition between 9.8 and 2.7 GPa, the boundary between orthorhombic and disordered forms of $NO^+NO_3^-$ can be estimated (see Fig. 6 and below).

Givan *et al.*[29] suggested based on low-temperature Raman data that nitrosonium nitrate exists as an amorphous material at ambient pressure and low temperature, but undergoes two phase transitions upon warming up, namely, the amorphous-crystalline phase-I transition at 169 K and crystalline phase-I to crystalline phase-II transition at 188 K. Therefore we also measured the temperature dependence of the x-ray diffraction at ambient pressure. When the temperature was increased stepwise from 80 to 185 K, no clearly identifiable diffraction pattern was evident, just as was found at 2 GPa and 80 K. We conclude that $NO^+NO_3^-$ remained amorphous or disordered.

IV. DISCUSSION

The density of $NO^+NO_3^-$ established by the equation of state gives important insight into the stability, thermodynamic properties, and the reaction mechanisms related to $NO^+NO_3^-$. Previous observations of the formation of $NO^+NO_3^-$ were either by temperature-induced transformation at ambient pressure or by photon-induced autoionization of molecular N_2O_4 at low pressures.[2–5] However, the symmetry-breaking transformation (or chemical reaction) from N_2O to $NO^+NO_3^-$ can be interpreted as being driven by the higher density of the product $NO^+NO_3^- + N_2$. Upon heating N_2O breaks down via two competing channels. Below 10 GPa, heating N_2O results in its dissociation into N_2 and O_2, while above 10 GPa, laser heating of the sample forms predominantly $NO^+NO_3^-$. The blocking of the disso-

ciation channel by high pressure strongly indicates that $NO^+NO_3^-$ is a more stable phase with lower free energy at high pressures. This observation, together with the density comparison, suggests that heating a mixture of N_2 and O_2 under pressure will directly produce $NO^+NO_3^-$, a result that has been confirmed.[23] Kinetic factors associated with these reaction channels should be investigated further. These results provide evidence that at high pressures $NO^+NO_3^-$ is a stable phase both at room temperature and high temperatures.

These observations provide a basis for extending the stability diagram of N_2O to high pressures and temperatures and provide useful information for understanding the formation of $NO^+NO_3^-$ from other species. At room temperature and ambient pressure, N_2O is a colorless gas and becomes fluid at 184 K, subsequently solidifying at 182 K. At low pressures and room temperature, N_2O forms the α phase ($Pa3$) below 4 GPa and β phase ($Cmca$) above 5 GPa. At intermediate pressures, x-ray-diffraction measurements indicate the coexistence of the two phases.[22] It is reported that the transition pressure between α and β has no significant temperature dependence. The melting point of N_2O was measured by Clusius *et al.*[24] to 0.025 GPa, and was extrapolated by Mills *et al.*[22] In the present study we also explored the melting curve at several other pressures using the resistance heating method. The melting was confirmed by both visual observation and Raman spectroscopy. We have refitted the melting curve with a Simon-type equation using both current measurements and those from Ref. 24 (Fig. 6). On heating, N_2O transforms to $NO^+NO_3^-$ and N_2 irreversibly at high pressure; it can dissociate into nitrogen and oxygen upon heating at other pressures. No attempt was made to study the reaction yield as a function of pressure and temperature. Several parallel heating experiments conducted at different pressures up to 40 GPa indicate that the transformation is complete and $NO^+NO_3^-$ is stable up to 2000 °C. The region where N_2O transforms to $NO^+NO_3^-$ is shown schematically in Fig. 6. We note that molecular N_2O was found to be stable up to 40 GPa and below 300 K (i.e., without heating).[25] Additional transformations at intermediate P-T conditions to form additional phases of molecular N_2O have been reported.[26]

The crystal structure of $NO^+NO_3^-$ at 21 GPa appears to be orthorhombic with four molecules per unit cell. By analogy to related ionic materials, a possible space group is $P2_1cn$.[6] In the present study, cell parameters were found to evolve smoothly over the entire pressure range from 9.9 to 32.2 GPa. This is consistent with IR and Raman measurements,[8] which likewise indicate that no major phase transitions occur in this pressure range. However, these spectroscopic data do reveal the presence of a transition below 10 GPa. The lowest pressure at which we observed x-ray diffraction at room temperature was 6.3 GPa. The diffraction pattern at this pressure differs significantly from those at higher pressures, such that the cell parameters are not consistent with the same orthorhombic structure. At 2.7 GPa, the diffraction peaks have become too weak to clearly identify, even when the sample was exposed to x-rays for a prolonged period. This weakening of the diffraction peaks may indicate that $NO^+NO_3^-$ at this pressure has an amorphous or disordered structure. Notably, it has been reported that at atmospheric pressure, $NO^+NO_3^-$ is predominantly in an amorphous phase.[27–30] We suggest that $NO^+NO_3^-$ transforms at room temperature from the orthorhombic structure to a disordered form on decompression from 9.8 to 2.7 GPa. This transition may be gradual, with intermediate ordered or partially ordered structures in between, making the boundary difficult to determine.

Finally, we comment on the low-temperature diffraction data and comparison with results from vibrational spectroscopy.[8] We observed that at ambient pressure $NO^+NO_3^-$ is stable below 180 K; at room temperature, it is stable above 1.0 GPa. Raising the temperature at ambient pressure or releasing the pressure at room temperatures results in the transformation of $NO^+NO_3^-$ into molecular N_2O_4. The estimated boundary between amorphous or disordered $NO^+NO_3^-$ and molecular N_2O_4 is indicated in Fig. 6. As described above, Givan *et al.*[29] suggested based on low-temperature Raman data that nitrosonium nitrate transforms from an amorphous phase to two crystalline phases at higher temperatures. One reason for the apparent discrepancy with previous observations could be due to kinetic factors in these two quite different experiments. The experiment of Givan *et al.*[29] involved ambient pressure N_2O_4 gas deposition, in which the deposition rate is critical for the transformation and characterization by vibrational spectroscopy. In contrast, the present study concerned decompression of $NO^+NO_3^-$ formed by laser heating of N_2O and x-ray diffraction. The $NO^+NO_3^-$ formed in such different ways may have distinct structures. Indeed, comparison of low-temperature Raman data[8] with previous studies[3,28] also suggests this conclusion. We observed abundant lattice modes at low temperature (80 K) and ambient pressure in our Raman spectra, in contrast to the results reported by Givan *et al.*[29] and Bolduan *et al.*[3] Moreover, at ambient pressure and temperature between 180 and 190 K, instead of a phase transition from crystalline phases I to II, our spectra indicate[8] that $NO^+NO_3^-$ transforms to molecular N_2O_4. The observation of abundant Raman excitations in the lattice mode region together with the weak diffraction pattern at low pressures suggest the $NO^+NO_3^-$ structure has long-range disorder but is partially ordered at short range. These results will be presented elsewhere.

V. CONCLUSIONS

We have conducted an x-ray-diffraction study of $NO^+NO_3^-$ at both room and low temperatures using synchrotron radiation facilities. Based on the orthorhombic structure previously determined by angle dispersive x-ray diffraction, we were able to derive the cell parameters from 9.9 to 32.2 GPa. The molecular volume has been fitted to the Birch-Murnaghan equation of state, from which the bulk modulus K_0 and its first derivative K_0' are determined to be 45.2($\pm$0.9) GPa and 3.18($\pm$0.90), respectively. Similar values were found using the Vinet equation of state. We find that the density for $NO^+NO_3^-$ is larger than both the assemblage of N_2+2O_2 and of $N_2O+3/2O_2$ indicating that the transformation to $NO^+NO_3^-$ is thermodynamically driven by pres-

sure. The room-temperature and low-temperature *in situ* x-ray-diffraction data, together with spectroscopic measurements, reveal new transformations and provide estimates of the phase relations for the system.

ACKNOWLEDGMENTS

This work was supported by funding received from Lawrence Livermore National Laboratory (LLNL) under Subcontract No. B515927 to Harvard University and by AFSOR and DARPA (F-49620-02-1-01859). We are grateful to J. Hu and Q. Guo for their assistance with the x-ray-diffraction measurements at beamline X17C and X17B of NSLS at Brookhaven National Laboratory.

[1] L. Parts and J. T. Miller, J. Chem. Phys. **43**, 136 (1965).
[2] F. Bolduan and H. J. Jodl, Chem. Phys. Lett. **85**, 283 (1982).
[3] F. Bolduan, H. J. Jodl, and A. Loewenschuss, J. Chem. Phys. **80**, 1739 (1984).
[4] S. F. Agnew, B. I. Swanson, L. H. Jones, R. L. Mills, and D. Schiferl, J. Phys. Chem. **87**, 5065 (1983).
[5] L. H. Jones, B. I. Swanson, and S. F. Agnew, J. Chem. Phys. **82**, 4389 (1985).
[6] M. Somayazulu, A. Goncharov, O. Tschauner, P. F. McMillan, H. K. Mao, and R. J. Hemley, Phys. Rev. Lett. **87**, 135504 (2001).
[7] V. Iota, C.-S. Yoo, and H. Cynn, Eos Trans. Am. Geophys. Union 82, Fall Meet, Suppl., Abstract T21B-0889 (2001).
[8] Y. Song, R. J. Hemley, Z. Liu, M. Somayazulu, H. K. Mao, and D. R. Herschbach, J. Chem. Phys. (to be published).
[9] F. Birch, J. Geophys. Res. **83**, 1257 (1978).
[10] P. Vinet, J. Ferrante, J. H. Rose, and J. R. Smith, J. Geophys. Res. **92**, 9319 (1987).
[11] H. K. Mao, J. Xu, and P. M. Bell, J. Geophys. Res. **91**, 4673 (1986).
[12] J. Z. Hu, H. K. Mao, Q. Z. Guo, and R. J. Hemley, *Science and Technology of High Pressure* (Universities Press, Hyderabad, India, 2000), pp. 1039–1042.
[13] H. Olijnyk, J. Chem. Phys. **93**, 8968 (1990).
[14] J. J. Dong (private communication).
[15] W. B. Holzapfel, Rep. Prog. Phys. **59**, 29 (1996).
[16] S. Desgreniers and K. E. Brister, *High Pressure Science and Technology* (World Scientific, Singapore, 1996), pp. 363–365.
[17] R. W. G. Wyckoff, *Crystal Structures*, Second Ed. (Wiley, New York, 1963), Vol. 1, pp. 371–372.
[18] R. E. Cohen, O. Gülseren, and R. J. Hemley, Am. Mineral. **85**, 338 (2000).
[19] B. Olinger, R. L. Mills, and R. B. Roof, Jr., J. Chem. Phys. **81**, 5068 (1984).
[20] A. Ruoff and S. Desgreniers, *Molecular Systems under High Pressure*, edited by R. Pucci and G. Piccitto (Elsevier, New York, 1991), p. 123.
[21] S. Johnson, M. Nicol, and D. Schiferl, J. Appl. Crystallogr. **26**, 320 (1993).
[22] R. L. Mills, B. Olinger, D. T. Cromer, and R. LeSar, J. Chem. Phys. **95**, 5392 (1991).
[23] Y. Ma, H. K. Mao, and R. J. Hemley (unpublished).
[24] K. Clusius, U. Piesbergen, and E. Varde, Helv. Chim. Acta **18**, 1290 (1960).
[25] H. Olijnyk, H. Daufer, M. Rubly, H.-J. Jodl, and H. D. Hochheimer, J. Chem. Phys. **93**, 45 (1991).
[26] C. S. Yoo (private communication).
[27] A. Givan and A. Loewenschuss, J. Chem. Phys. **90**, 6135 (1989).
[28] A. Givan and A. Loewenschuss, J. Chem. Phys. **91**, 5126 (1989).
[29] A. Givan and A. Loewenschuss, J. Chem. Phys. **93**, 7592 (1990).
[30] A. Givan and A. Loewenschuss, J. Chem. Phys. **94**, 7562 (1991).
[31] E. H. Abramson, L. J. Slutsky, M. D. Harrell, and J. M. Brown, J. Chem. Phys. **110**, 10493 (1999).